

Enhancing School Zone and School Bus Safety



SAFETY RESEARCH USING SIMULATION

UNIVERSITY TRANSPORTATION CENTER

Jaeyoung Lee, Ph.D., PI
Assistant Professor and Safety Program Director

Mohamed Abdel-Aty, Ph.D., P.E., Co-PI
Pegasus Professor & Chair

Md Hasibur Rahman

PhD Student

Enhancing School Zone and School Bus Safety

Jaeyoung Lee, Ph.D., PI

Assistant Professor and Safety Program Director

Center for Advanced Transportation Systems Simulation

Department of Civil, Environmental and Construction Engineering

University of Central Florida

<http://orcid.org/0000-0003-1211-688X>

Mohamed Abdel-Aty, Ph.D., Co-PI

Pegasus Professor & Chair

Department of Civil, Environmental and Construction Engineering

University of Central Florida

<http://orcid.org/0000-0002-4838-1573>

Md Hasibur Rahman

Ph.D. Student

Department of Civil, Environmental and Construction Engineering

University of Central Florida

<http://orcid.org/0000-0001-5387-7365>

A Report on Research Sponsored by

SAFER-SIM University Transportation Center

Federal Grant No: 69A3551747131

August 2018

DISCLAIMER

The contents of this report reflect the views of the authors, who are responsible for the facts and the accuracy of the information presented herein. This document is disseminated in the interest of information exchange. The report is funded, partially or entirely, by a grant from the U.S. Department of Transportation's University Transportation Centers Program. However, the U.S. Government assumes no liability for the contents or use thereof.

Table of Contents

Table of Contents	v
List of Figures	vii
List of Tables	viii
Abstract	ix
1 Introduction	0
2 Literature Review	1
2.1 Speeding in School Zones	1
2.2 Effectiveness of Various Signs in School Zones	1
2.3 Environmental and Geometric Design	3
3 Selection of the Study Area	5
3.1 Data Collection	5
3.2 Data Processing	5
4 Microsimulation Network	8
4.1 Data collection	8
4.2 Network Building in VISSIM	10
4.2.1 Microsimulation Area	10
4.2.2 Network Coding	10
4.2.3 Traffic Data Input	12
4.2.4 VISSIM Network	16
4.3 Calibration	16
5 Proposed Methodologies	19
5.1 Two-Step Speed Reduction (TSR)	19
5.2 Decreasing the Number of Driveways (DD)	20
5.3 Replace TWLTL with Raised Median (RM)	22
6 Surrogate Measures of Safety	23
7 Results and Discussion	26
8 Summary and Conclusion	34
9 Follow-up Research Topics	35

References36

List of Figures

Figure 1.1 - Previous crash statistics in school zones in the United States (source: FARS data)	0
Figure 3.1 - Total Crashes of the Ten School Zones	6
Figure 3.2 - DVMT of the Ten School Zones.....	7
Figure 3.3 - Crash Rate of the Ten School Zones	7
Figure 4.1 - Vehicle Composition in the Morning and Afternoon.....	8
Figure 4.2 - Vehicle Composition Eastbound and Westbound	8
Figure 4.3 - Vehicle Composition by Morning and Afternoon for Eastbound and Westbound	9
Figure 4.4 - Directional Distribution during Morning and Afternoon	9
Figure 4.5 - Microsimulation Area	10
Figure 4.6 - Description of Link in VISSIM	11
Figure 4.7 - Roadway Segments Coded in VISSIM	12
Figure 4.8 – Two-Way Left-Turn Lane in VISSIM.....	12
Figure 4.9 - Hourly Traffic Volume	13
Figure 4.10 - CDF of PC and HV/SB on South John Young Pkwy	14
Figure 4.11 - Desired Speed Distribution in VISSIM.....	15
Figure 4.12 - Data Collection Points in VISSIM.....	16
Figure 4.13 - Microsimulation Network in VISSIM.....	16
Figure 5.1 - Two-Step Speed-Reduction Procedure	19
Figure 5.2 - Reducing Driveway Access.....	21
Figure 5.3 - TWLTL to Raised Median	22
Figure 7.1 - Average Value of TET, TIT and TERCRI for All Sub-scenarios.	26
Figure 7.2 - Distribution of TET (a), TIT (b), TERCRI (c) for the Best Three Sub-scenarios with Base Scenarios and the Value of TET, TIT, TERCRI for the Best Three Sub-scenarios with Base Scenario (d). ...	33

List of Tables

Table 2.1- Criterion for establishing school speed limits.....	1
Table 3.1- Top Ten Schools Based on Crash Rate	5
Table 7.1 - Summary Statistics of TET and TIT	27
Table 7.2 - Summary Statistics of TERCRI	28
Table 7.3 - One-Way ANOVA Analysis of TET, TIT, and TERCRI.	29
Table 7.4 - Sensitivity Analysis of Different Values of TTC Threshold.....	31
Table 7.5 - Sensitivity Analysis of TET	31
Table 7.6 - Sensitivity Analysis of TIT	32

Abstract

Safety issues in school zone areas have been one of the most important topics in the traffic safety field. This research project assesses the safety effects of different roadway countermeasures in school zone areas. Although many studies have evaluated the effectiveness of various traffic control devices (e.g., sign, flashing beacon, speed monitoring display), there is a lack of studies exploring different roadway countermeasures that might have significant impacts on the school zone safety. In this research project, the most crash-prone school zone was identified in Orange and Seminole Counties, Florida, based on crash rate, which is defined as crash per thousand daily vehicle miles traveled. The results showed that Westridge Middle and Sadler Elementary schools were the top two crash-prone school zones. Afterward, a microsimulation network was built in VISSIM to test different roadway countermeasures in the school zones. Before applying different countermeasures, the network was calibrated and validated by traffic volume and travel time in order to replicate the real field. Three different countermeasures—two-step speed reduction, decreasing the number of driveways, and converting the two-way left-turn lane (TWLTL) to a raised median—were implemented in microsimulation and compared with the field condition. For each countermeasure, we also ran different sub-scenarios. In two-step speed reduction, we analyzed three sub-scenarios that were defined by the maximum speed limit on the main roadway. The number of driveways was reduced by 25%, 50%, 75%, and 100%, so four sub-scenarios were used to analyze in this countermeasure. We replaced TWLTL with a raised median, so all the left-turning vehicles made left turns either at the intersection or median. Therefore, two sub-scenarios, intersection U-turn and median U-turn, were analyzed. Surrogate safety measures are widely used as indicators to evaluate crash risk in the microsimulation software as it cannot directly measure the traffic crashes. In this research project, three surrogate safety measures were used; two of them were developed from time-to-collision (TTC) notations. Three surrogate safety measures—time-exposed time to collision (TET), time-integrated time to collision (TIT), and (3) time-exposed rear-end crash risk index (TERCRI) —were utilized in this research project as indicators for safety evaluation. The higher value of surrogate safety measures indicates higher crash risk. The results showed that all the sub-scenarios in two-step speed reduction and decreasing driveway access reduced TET, TIT, and TERCRI values significantly compared to the base condition. Moreover, the combination of two-step speed reduction and decreasing driveway access countermeasures outperformed their individual effects as well as the base condition. The one-way ANOVA analysis showed that all the sub-scenarios were significantly different from each other. Sensitivity analysis was also conducted to capture the impact of different sub-scenarios for different values of TTC threshold. The results show that all the sub-scenarios in two-step speed reduction and decreasing the number of driveway access reduced TET, TIT, and TERCRI values significantly for different values of TTC threshold, which ranged from 1 to 3 s. Conversely, for converting the TWLTL to the raised median, the crash risk was higher than the base condition because the value of TET, TIT, and TERCRI was much higher than the base condition. Therefore, the results of this research project provide useful insights for transportation and safety planners.

1 Introduction

Traffic crashes are a serious safety concern, and they are even more serious when they involve school-age pedestrians. There has been an increase in the number of school-age pedestrians and cyclists injured and killed throughout the years, and many states have set a lower speed limit in school zones to protect children from severe crashes. However, drivers often do not comply with these speed limits. Some school zones require drivers to reduce their speed suddenly, which may cause a large variation in speed between vehicles and may result in rear-end crashes. The crash statistics near school zones in the US are given in Figure 1.1.

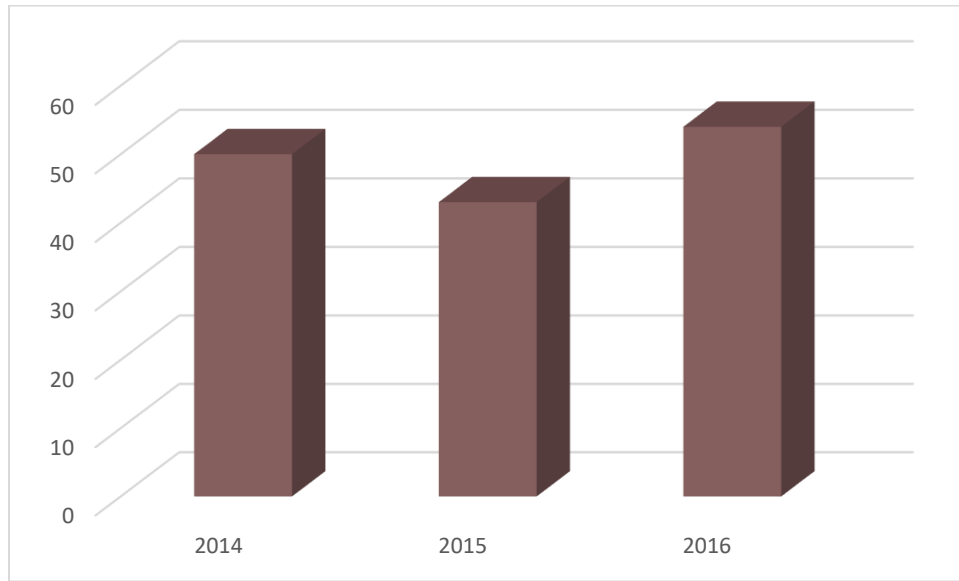


Figure 1.1 - Previous crash statistics in school zones in the United States (source: FARS data)

Figure 1.1 shows that fatal crashes in school zones are high and that there is an increasing trend, which means school zone safety should be a focus. Therefore, the objectives of this research are

- To analyze driving behavior and countermeasures in the reduced speed limits in school zones; and
- To investigate the impacts of geometric design of roadways and the number of driveways on safety in school zones.

2 Literature Review

2.1 Speeding in School Zones

The impact of speeding is acute with the presence of a high percentage of vulnerable road users [1] and school zones are the most prominent of them [2]. Furthermore, child pedestrian crashes are more likely to happen closer to school zones than farther away [3,4].

Ellison et al. [5] examined speeding behavior in school zones in Sydney, Australia, by using the Global Positioning System (GPS). They observed 147 drivers over five weeks and focused on both the duration and magnitude of speeding. The results showed that over 20 percent of the distance driven in school zones was at a speed higher than the posted speed limit (40 km/h) and 8 percent was driven at 10 km/h or more above the speed limit. Also, the study implied that speeding rate in school zones is higher than on urban arterials and residential streets. In addition, Roper et al. [2] found that approximately half of all vehicles exceeded the speed limit, and Kattan et al. [6] showed that around 10% of the vehicles exceeded the speed limit by 10 km/h or more above the posted speed limit.

A posted speed limit in school zones depends on the roadway characteristics on which the school is located and the segments of the roadway before the school zones start [5]. This study also showed that if the speed of the previous segment was higher than 70 km/h then it was difficult to reduce the speed to the posted speed limit (40 km/h). McCoy and Heimann [7] also showed that the school zone speed limit depends not only on an effective signing and marking system but also on a reasonable speed limit and the preceding roadway segments. For this reason, the paper provided criterion for establishing school zone speed limits as follows (Table-2.1).

Table 2.1- Criterion for establishing school speed limits

Distance of school building from Roadway (feet)	Approach Speed Limit (mph)		
	25	35-45	55
0-55	20	20	30
56-100	25	25	30
Over 100	25	30	35

2.2 Effectiveness of Various Signs in School Zones

A traffic sign is one of the most effective tools for controlling drivers' actions. It is also used to deliver warning and advice to drivers. A failure to regulate driver behavior is considered a major contributor to road traffic crashes [8]. This situation is worse in school zone areas due to the presence of children.

Saibel et al. [9] evaluated the effects of the various types of signs on drivers' speed in a school zone in Washington State. They measured the vehicle speeds in the school zone 30 minutes before the start of school and 30 minutes after the end of school. The school speed limit was 20 mph for all sites, and the project included 38 study sites. The sites were divided by the posted speed limit for the road, either 25 mph or 30 mph and greater, and the type of sign:

- Time of day: the sign indicates that the school speed limit is in effect for all hours of the day or specific times of the day, e.g., 7:30 a.m. to 4:30 p.m.
- Flashing beacon: the sign indicates that a speed limit of 20 mph is in effect when the beacon is flashing.
- When present: the sign indicates that the 20 mph speed limit is active when children are present.
- When flagged: the sign indicates that the speed limit will be reduced when orange flags are attached to the sign post.

The result showed that there was no statistical difference for various signs with a posted speed limit of 25 mph, but for the roads with a posted speed limit of 30 mph or greater, the average speed was higher with the "when children are present" and "when flagged" signs. In contrast, flashing beacon signs resulted in a significantly lower speed of 22.5 mph, which is 5-7 mph slower than those resulting from the other signs.

Flashing beacons are mainly used to indicate the "Begin school zone" sign and are required in some states. Rear-facing beacons are normally used at either end of the school zone to serve as a reminder of the end of a school zone as drivers often do not understand whether they are in the school zone area or not. So, a study was conducted in College Station, Texas, to determine the effectiveness of rear-facing school speed limit beacons to reduce the speed limit as sometimes drivers might forget that they are in the restricted speed area when the school zone length is long. The study was conducted at four separate sites before and after the installation of the beacons, and the results showed that speed was reduced at three of the sites. The site that experienced no change in speed compliance was the zone with no intersections and was of a normal length. So, we can conclude that rear-facing flashing beacons can reduce speed in school zones with substantial length [10].

In a study of differential effects of traffic signs in school zones in New South Wales, Sydney, Australia [11], it was found that the combination of written text and flashing lights was the most effective in reducing vehicle speed in a 40 km/h speed limit when drivers were interrupted by signalized intersections. It was also found that a sign with flashing lights only could reduce the speed but not below the posted speed limit. There was no difference between the text-only and no-sign conditions. Another study was conducted in North Carolina about the effectiveness of school zone flashers and found no practical difference in vehicle speed between flasher and non-flasher locations during school time hours [12].

A speed monitoring display (SMD) provides actual feedback to drivers on their actions within the school zone. It also shows the drivers both the posted speed limit and the speed at which they are traveling. In South Korea, a study was conducted to evaluate the effectiveness of SMD to reduce the speed in a school zone area. The selected study location had high visibility,

low congestion, and no presence of other signals in order to evaluate the sole effect of an SMD. The study also investigated the short- and long-term effects of SMDs and found that an SMD can reduce speed more in the short term than the long term. However, in both cases, the speed was lower than in the previous condition [13]. The average speed reduction was about 17.5% (8.2 km/h) and 12.4% (5.8 km/h) for the short-term and long-term studies, respectively. Another study on utilizing SMDs conducted in Utah in 2005 found that safety and efficiency vary by location and that SMDs can reduce speed without a negative impact on the safety of a location [14]. Moreover, a study was conducted to measure the effectiveness of dynamic speed display signs (DSDSs) in school zones [15]. The main result of this study was that speeds were reduced by 9 mph at the school speed zone where DSDSs were present, but that it can be more effective if appropriate site conditions apply.

There is another way by which we can influence driver behavior through interactive traffic signs and devices. A study conducted by the National Highway Traffic Safety Administration (NHTSA) in Portland, Oregon, determined how automated speed enforcement (ASE) impacted speed-reduction efforts in school zones and how the public accepted and perceived their presence [16]. Automated speed enforcement measures the vehicle speed and, if the speed is higher than the posted speed, will automatically give a ticket to the violators. School speed limits in Oregon are 20 mph, and this study used ASE in five different school zones two to three times a week for a three-month period during the school year. The results were compared to five school zones where there was no ASE present. The result showed that average speed dropped when ASE was present when the flashing beacon was on or off. This drop was 3-4 mph more when the flashing beacon was on. Therefore, it can be concluded that ASE dropped the vehicle speed and that it is more effective when paired with a flashing beacon.

Zhao et al. [17] conducted a study in China to examine the effectiveness of traffic control devices on driver behavior. This research used a driving simulator experiment to assess the effect of school zone signs and markings for two different types of schools. Average speed, relative speed difference, standard deviation of acceleration, and 85th percentile speed were used to evaluate the effectiveness of traffic control devices, which were derived from a driving simulator. The results showed that a flashing beacon with a “school crossing ahead” warning and a “school crossing ahead” warning with school crossing pavement markings were recommended for school zones adjacent to a major multilane roadway characterized by high traffic volume and a median strip. It also showed that “school crossing ahead” pavement markings were recommended for a minor two-lane roadway.

2.3 Environmental and Geometric Design

There are various physical and social attributes that regulate the child pedestrian–vehicular crashes in school zones. Children are more exposed in school zones and thus increase pedestrian crashes. Walking rates are higher among lower socio-economic groups [33], so children from lower-income groups have to walk to and from school, which increases the probability of pedestrian crashes. Clifton and Kreamer-Fulfs [19] examined pedestrian-vehicular crashes in the vicinity of public schools, the severity of injuries sustained, and their relationship to the physical and social attributes near the schools. In this case, they developed multivariate models of crash severity and crash risk exposure as a function of the social and physical characteristics of the areas surrounding schools in Baltimore, Maryland. Results showed that the presence of a

driveway or turning bay at the school entrance decreased crash occurrence and severity and that the presence of recreational facilities increased crash occurrence and severity in Baltimore City, Maryland.

Ben-Bassat and Shinar [20] investigated the effect of shoulder width, guardrail, and roadway geometry on driver perception and behavior. They found that shoulder width does not affect actual speed but if a guardrail is present at the right edge of the shoulder, it increases driving safety. Tay [13] also found that the width of the roadway and the presence of fencing makes drivers comfortable and causes them to drive at higher speeds. This study also showed that compliance rate is higher for two-lane roads than for four-lane roads. This is because more lanes give drivers more room to drive and hence increase the probability of crash. However, Strawderman et al. [22] showed a different result. In their study, the authors measured the compliance rate for both high- and low-saturation school zones. The results implied that compliance rate is higher for four-lane high-saturation zones than for two-lane high-saturation zones (46.79% to 20.19%). However, in the case of low saturation, four-lane compliance is higher than two-lane compliance, but the difference is small (7.23% to 2.56%).

Although the existing studies and established guidelines provide useful information regarding different traffic control devices in school zones, very few studies investigated the effect of different roadway countermeasures in school zones. So, the objective of this research is to find the effectiveness of different roadway characteristics, i.e., two-step speed reduction, decreasing the number of driveways, etc., in school zones and measure traffic safety by using microsimulation software. Furthermore, in most of the previous studies [12,23], traffic control devices were installed in school zones and the authors measured their effectiveness. Sometimes, there was no significant improvement of safety in the school zone by implementing this change. Hence, to address this problem, we analyzed the impact of different roadway characteristics in a microsimulation environment, which can give a quick and efficient indication of the safety effectiveness to transportation planners or engineers prior to implementing them.

3 Selection of the Study Area

3.1 Data Collection

In order to identify the most crash-prone school zone in Orange and Seminole Counties in Florida, we collected school location data, annual average daily traffic (AADT), and total crashes for the years 2012-2016 from Signal four Analytics (S4A) , managed by the University of Florida GeoPlan Center.

3.2 Data Processing

A school zone is defined by creating a 1000 ft. buffer zone around a school. In this case, we have selected only public schools in Orange and Seminole Counties in Florida. Sometimes two or more school zones overlapped each other, so we merged the overlapping school zones and counted them as one zone. Furthermore, we selected the AADT inside the buffer area only. Hence, to identify the most crash-prone school zone, we used crash rate, which is defined as total crashes per daily vehicle miles (in 1000) traveled (DVMT) within the school zone. First, the number of crashes were counted inside the buffer area of a school, which was further filtered by creating a 200 ft. radius along the length of only those roadways that had AADT value. Moreover, to calculate the DVMT, we multiplied the AADT values with segment length in miles within a school zone. The above process was continued separately in the case of multiple roadway segments, and then the totals were combined to calculate DVMT. Hence, the total number of crashes inside the buffer area was then divided by the DVMT for each school zone to find the crash rate. We excluded those schools where there was no roadway segment inside the buffer area because, in this case, DVMT was equal to zero. Finally, we identified the top ten school zones based on crash rate, as shown in Table 3.1.

Table 3.1- Top Ten Schools Based on Crash Rate

Name	Type	Total Crash	DVM	Crash Rate	Overlapped
Westridge Middle	Middle	248	9204	26.943	Yes
Sadler Elementary	Elementary				
Innovations Middle School	Middle/Jr. High	411	19145	21.467	
Aloma Elementary	Elementary	333	19451	17.119	
Pine Hills Elementary	Elementary	50	2930	17.059	
Oak Hill Elementary	Elementary	416	26405	15.754	Yes
Sunshine High Charter	Senior High				
Union Park Elementary	Elementary	415	27418	15.136	Yes

Union Park Middle	Middle				
Howard Middle	Middle	199	13314	14.946	

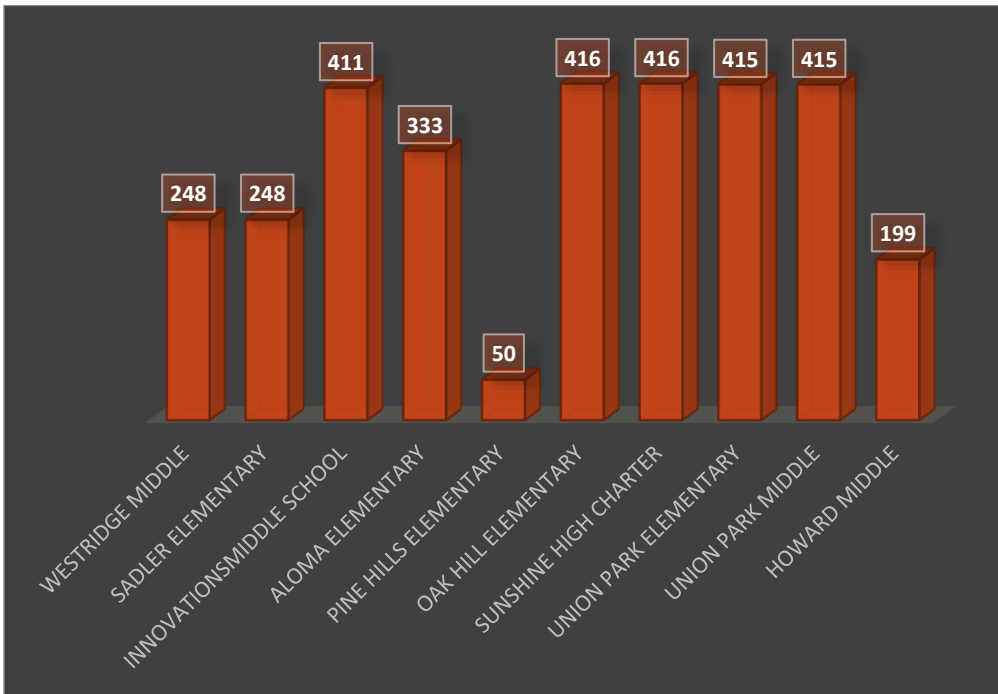


Figure 3.1 - Total Crashes of the Ten School Zones

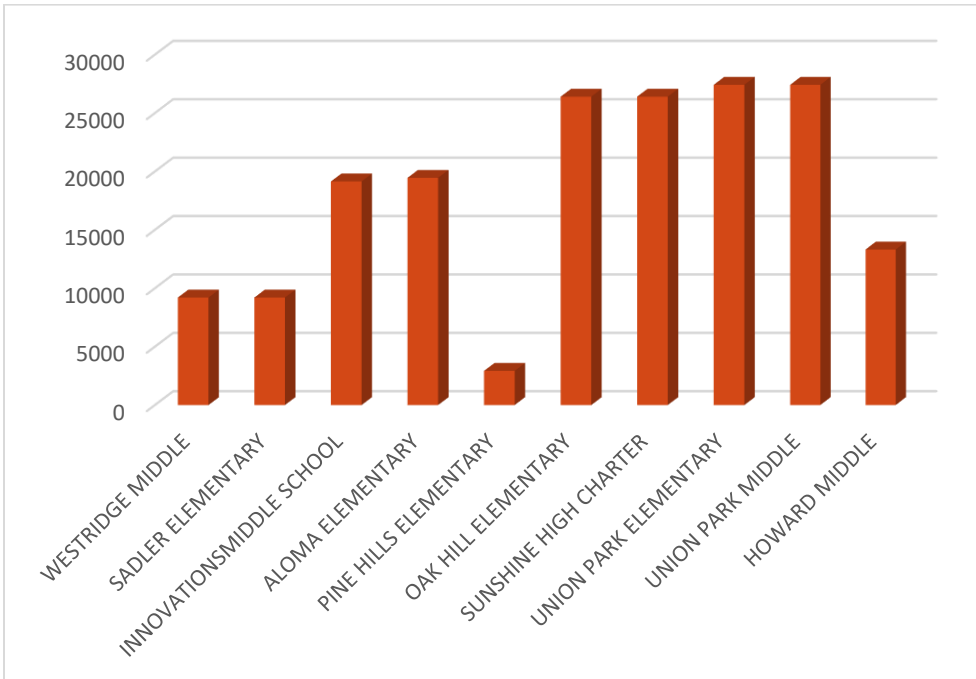


Figure 3.2 - DVMT of the Ten School Zones

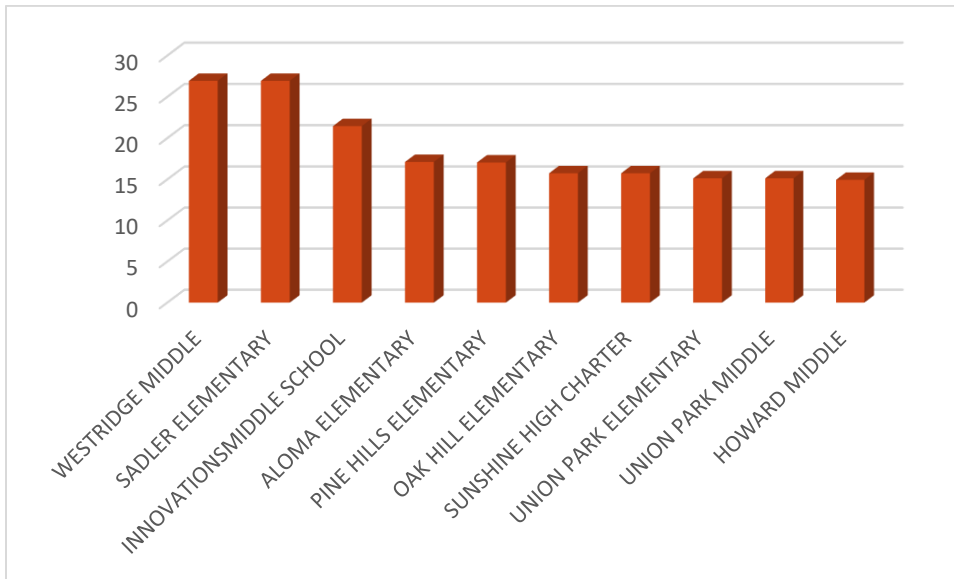


Figure 3.3 - Crash Rate of the Ten School Zones

Crash rate is higher for those school zones where the number of crashes is larger and DVMT is smaller. According to Figure 3.1 and Table 3.1, the school zones with the highest crash rates are Oak Hill Elementary and Sunshine High Charter School. The lowest DVMT was observed at Pine Hills Elementary and Westridge Middle School (Figure 3.2). Finally, we found the highest crash rate at Westridge Middle School and Sadler Elementary School (Figure 3.3), and the school zone of these two schools was selected as the study area.

4 Microsimulation Network

4.1 Data collection

In order to obtain traffic volume data from the main corridor (West Oak Ridge Road), the research team conducted a volume study survey in the school zones. The team collected data for two time periods: morning (7:20 to 8:30 a.m.) and afternoon (2:55 to 3:55 p.m.) on a Thursday in two different locations. The research team counted three types of vehicles separately (i.e., passenger car (PC), heavy goods vehicles (HV), and school buses (SB)). The composition of each vehicle type is presented in Figure 4.1.

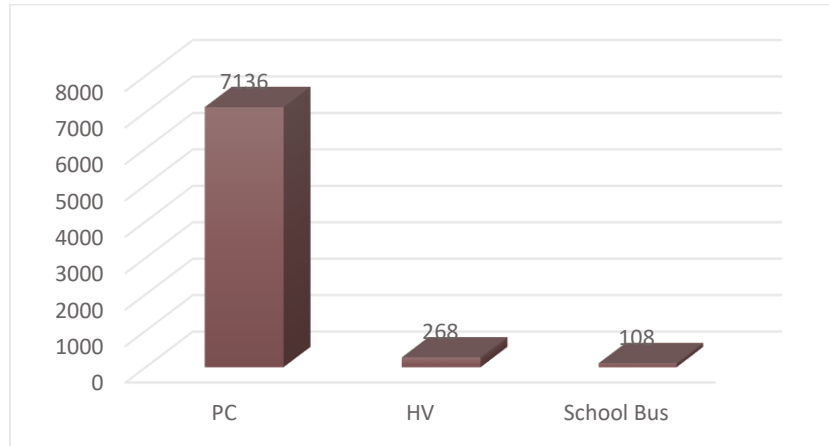


Figure 4.1 - Vehicle Composition in the Morning and Afternoon

Figure 4.1 shows that the total of the traffic volume in both directions on the roadway was 7,512 and that the number of PCs was significantly higher than the other two types. The percentage of PCs was around 95%, and those of HVs and SBs were 3% and 2%, respectively.

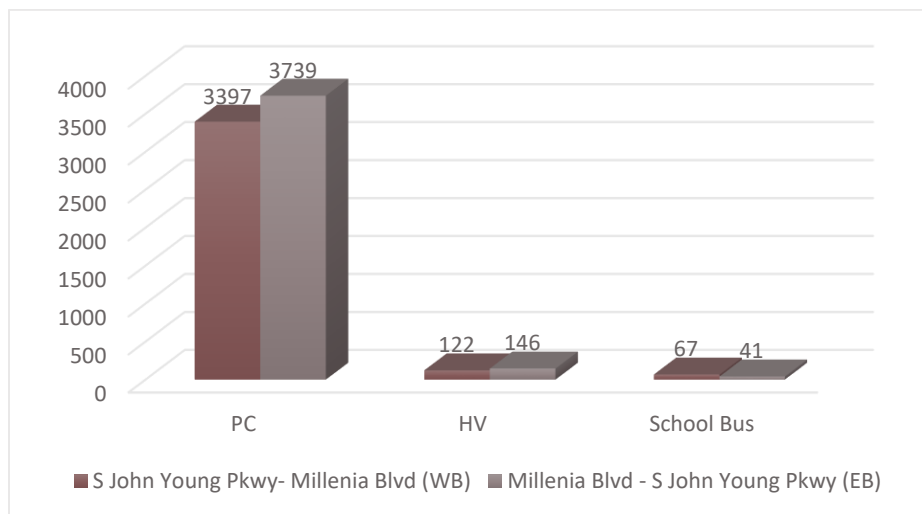


Figure 4.2 - Vehicle Composition Eastbound and Westbound

Figure 4.2 presents the vehicle composition by direction (eastbound and westbound). As shown in the figure, the total number of PCs and HVs was larger for eastbound (Millenia Boulevard - South John Young Parkway) than westbound (South John Young Parkway - Millenia Boulevard). On the other hand, the number of SBs was larger for westbound.

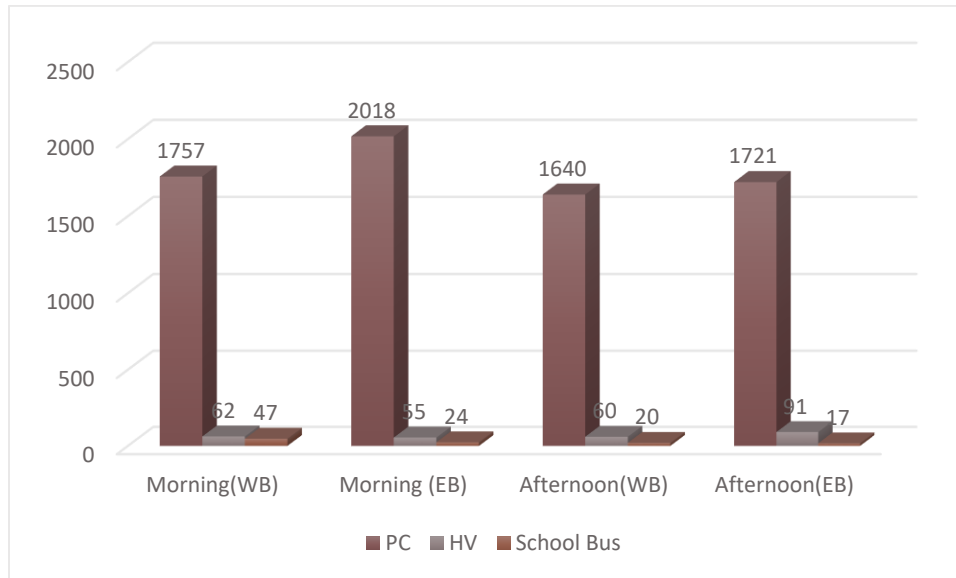


Figure 4.3 - Vehicle Composition by Morning and Afternoon for Eastbound and Westbound

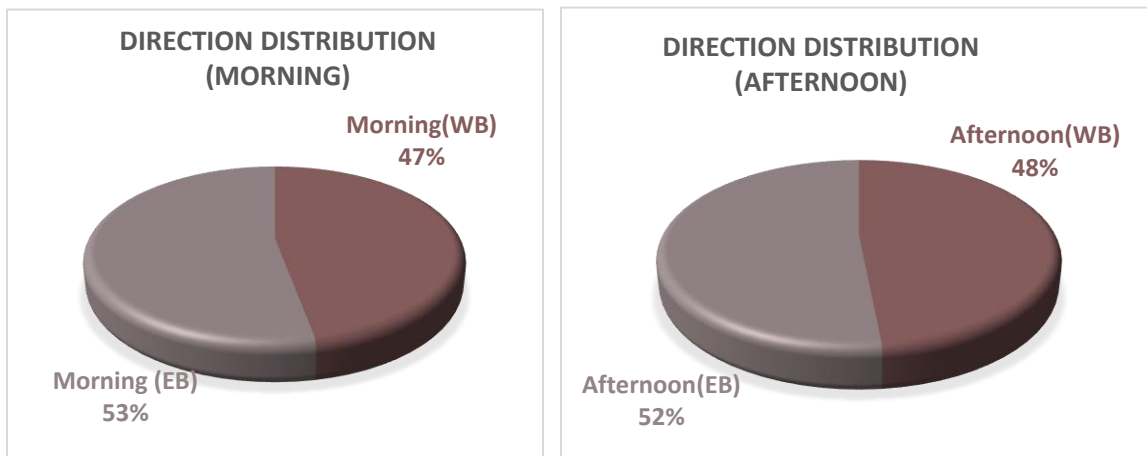


Figure 4.4 - Directional Distribution during Morning and Afternoon

In general, traffic volume is much larger in one direction than the other during morning peak hours, and the reverse scenario occurs during afternoon peak hours. However, the above analysis shows that the directional distribution of traffic volume was almost the same during the morning and afternoon, which means that the flow was almost constant in both directions in both the morning and the afternoon (Figures 4.3 and 4.4).

Also, the research team analyzed the percentage of traffic volume with respect to AADT and found that the percentage varied from 4-6% of AADT during the morning and afternoon periods.

4.2 Network Building in VISSIM

4.2.1 Microsimulation Area

According to the U.S. DOT microsimulation guideline for arterials [24], the model network should extend at least one intersection beyond those within the boundaries of the improvement, and it should include areas that might be impacted by the proposed improvement strategies. As the main objective of this project is to improve school zone safety, the research team selected the roadways (i.e., West Oak Ridge, Millenia Boulevard, South John Young Parkway, etc.) near the school zone that might have a major impact on school zone safety. Hence, the team developed a network in VISSIM that was about 3.21 miles long on West Oak Ridge Road and connected with South John Young Parkway (1.7 miles long). Moreover, the team considered around 29 driveway accesses and 7 intersections that might have impacts on the main roadway as well as the school zone. The proposed full network in VISSIM is shown in Figure 4.5.

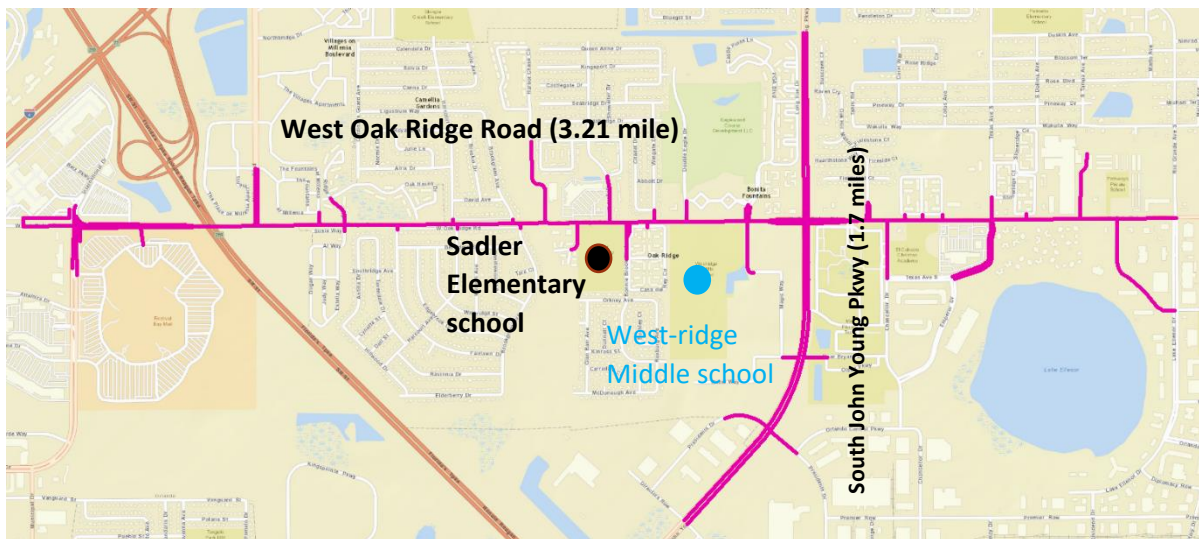


Figure 4.5 - Microsimulation Area

4.2.2 Network Coding

In VISSIM, there are two basic components of a roadway network: links and connectors. The links represent roadway segments and are connected to other links by connectors. Thus, vehicles cannot travel from one link to another without connectors attached. There are several properties that must be specified for each link: (1) number of lanes for the segment; (2) behavior type—there are six types of behavior in total, and urban (motorized) was selected in this project; (3) lane width, which was set as 12.0 feet; and (4) gradient, set as 0% since the study segment is flat. Following the roadway shapes in the background Bing map, which is toggled in VISSIM, the research team adjusted the curvatures of the studied segment by coding through adjusting the shape of links and connectors. Finally, the model of the arterial segment could accurately represent the geometric characteristics of the studied arterial segment. Figure

4.6 displays the link description in VISSIM, and Figure 4.7 shows the roadway segments coded in VISSIM with the background map where links are indicated with a blue line and connectors are indicated with red.

Link ? X

No.: Name:

Num. of lanes: Behavior type: 1: Urban (motorized) v

Link length: 237.636 ft Display type: 1: Road gray v

Level: 1: Base v

Is pedestrian area

Lanes Display Others

Count	Index	Width	BlockedVel	DisplayTyp	NoLnChLA	NoLnChRA	NoLnChLV	NoLnChRV
1	1	12.00			<input type="checkbox"/>	<input checked="" type="checkbox"/>		
2	2	12.00			<input type="checkbox"/>	<input type="checkbox"/>		
3	3	12.00			<input checked="" type="checkbox"/>	<input type="checkbox"/>	<input checked="" type="checkbox"/>	

Has overtaking lane

OK Cancel

Figure 4.6 - Description of Link in VISSIM

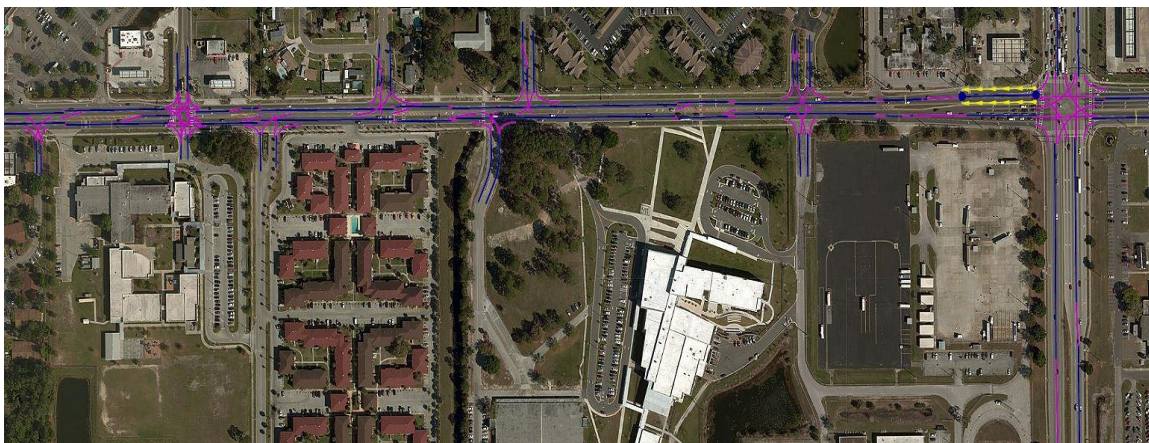


Figure 4.7 - Roadway Segments Coded in VISSIM

Also, the research team used priority rules, stop signs, and conflict areas tools for coding TWLTL in VISSIM, as shown in Figure 4.8.



Figure 4.8 – Two-Way Left-Turn Lane in VISSIM

4.2.3 Traffic Data Input

Traffic data, i.e., volume, vehicle composition, and speed, are needed in addition to the roadway geometric characteristics, links, and connectors. Nevertheless, there was no detector to collect real-time traffic volume data in the study area. Therefore, in order to input the traffic volume in each roadway in VISSIM, the research team used the traffic volume percentage with respect to AADT that was found for West Oak Ridge Road from the volume study survey and multiplied this value with the AADT of the connecting roadways. Because the team collected data from two different locations, two different traffic volume percentages with respect to AADT were estimated and were further used to calculate the hourly traffic volume of each roadway. Figure 4.9 displays which percentages were used for which roadways.

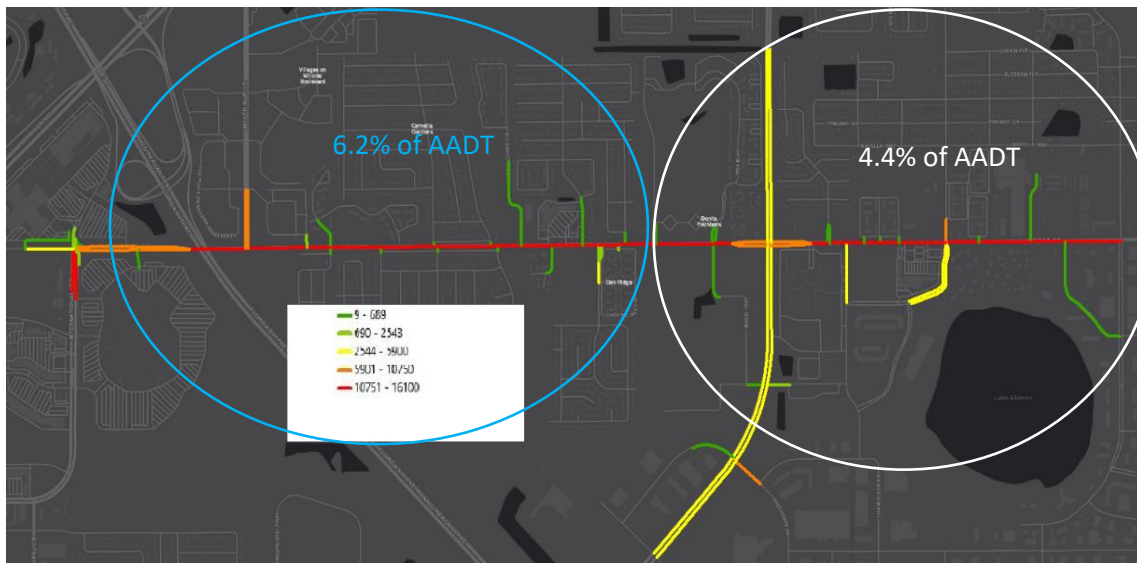


Figure 4.9 - Hourly Traffic Volume

In Figure 4.9, the blue and white circles indicate that 6.2% and 4.4%, respectively, of AADT were used to calculate hourly traffic volume of each roadway bounded by the circle. Also, the team ranked roadways by traffic volume; the green marker indicates low traffic volume, and the red marker indicates high traffic volume roads.

The simulation time was from 7:00 to 9:00 a.m., and the first and last 30 minutes were selected for warm-up and cool-down periods. The traffic data was aggregated by 5-minute intervals for input into the VISSIM, and a similar vehicle composition (95% PCs, 3% HVs, 2% SBs) was used for all roadways.

Desired speed is the speed when drivers are not hindered by other vehicles or network objects [25]. Getting desired speed distribution information is difficult because vehicles are always hindered by other vehicles in the roadway. A better way to get desired speed is to find the off-peak hours when traffic volume is low. At low volume, vehicles are less likely to be hindered by other vehicles and are able to maintain their desired speed.

Because of the unavailability of real-time traffic volume data, the research team was not able to differentiate peak and off-peak hours for our study area. Therefore, the team assumed that the off-peak period was 12:00 to 2:00 a.m. Hence, the team collected speed data from HERE, National Performance Measure Research Data Set (NPMRDS), which provided the aggregated speed of vehicles per 1-minute interval, which was further aggregated by 5-minute intervals for the analysis.

In order to formulate cumulative speed distribution, the research team used the coefficient of variation (CV), mean speed, and standard deviation of speed. Hjälmdahl and Várhelyi [26] showed that in an arterial, the standard deviation of speed was around 5.31 when the mean speed was about 50 mph. The CV was estimated by using this value. Then the team calculated the standard deviation of speed for the dataset using the above CV and the mean value of speed from the HERE dataset.

Moreover, HERE data provided the average speed for all types of vehicles, i.e., PCs, HVs, and others. However, VISSIM had to specify the desired speed distributions for different vehicle types. Therefore, one assumption was made to calculate the desired speed distributions: the average speed of a PC was 6 mph higher than that of an HV [27], and the speed of HVs and SBs was the same.

From the field data, it was found that the percentage of PCs in the study segment was about 95%. Supposing x is the speed of PCs, then the speed for HVs or SBs is equal to $(x-6)$, and the average speed provided by HERE is y . Then,

$$0.95x + 0.05(x-6) = y \dots\dots\dots (4.1)$$

From Equation 4.1, the PC speed was found to be about $(y+0.3)$, and the HV or SB speed was around $(y-5.7)$. Then the desired speed distribution of PCs and HVs or SBs were acquired separately. Figure 4.10 gives an example of the desired speed distribution for PCs and HVs/SBs

eastbound on the South John Young Parkway. Also, the input of the desired speed distribution in VISSIM is shown in Figure 4.11.

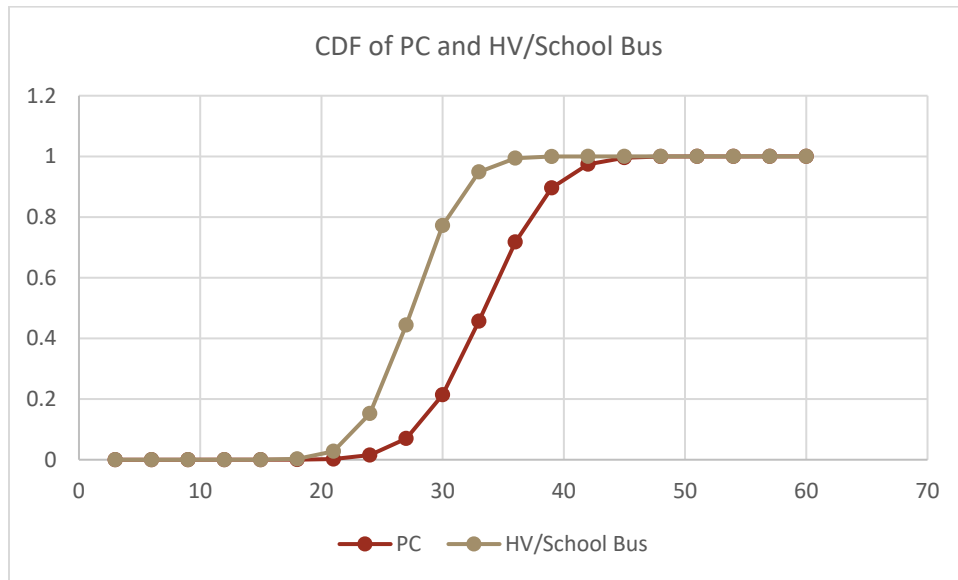
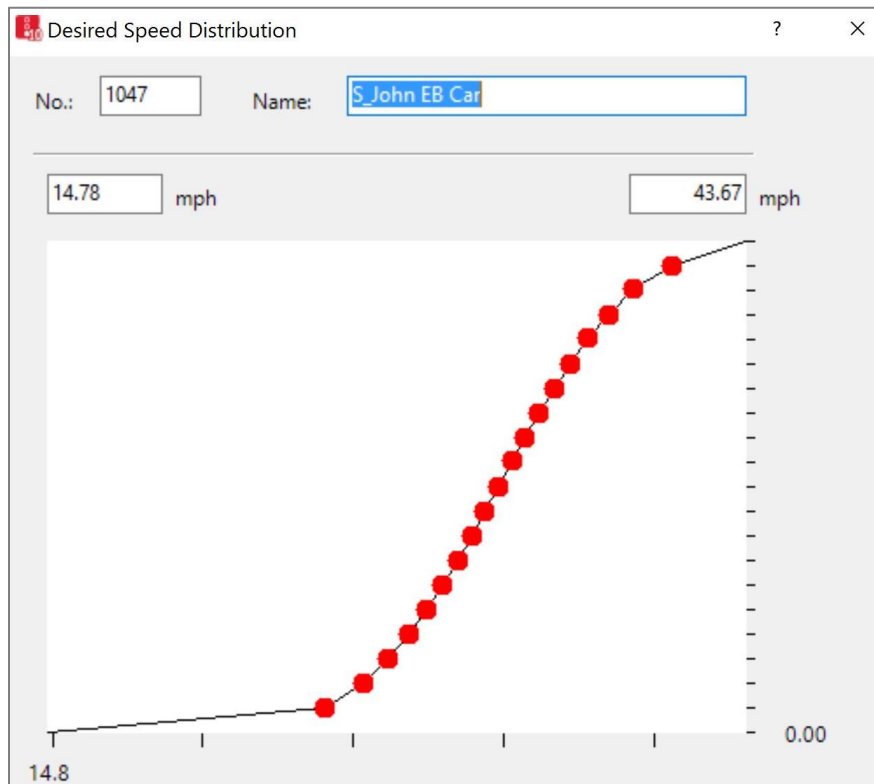


Figure 4.10 - CDF of PC and HV/SB on South John Young Pkwy



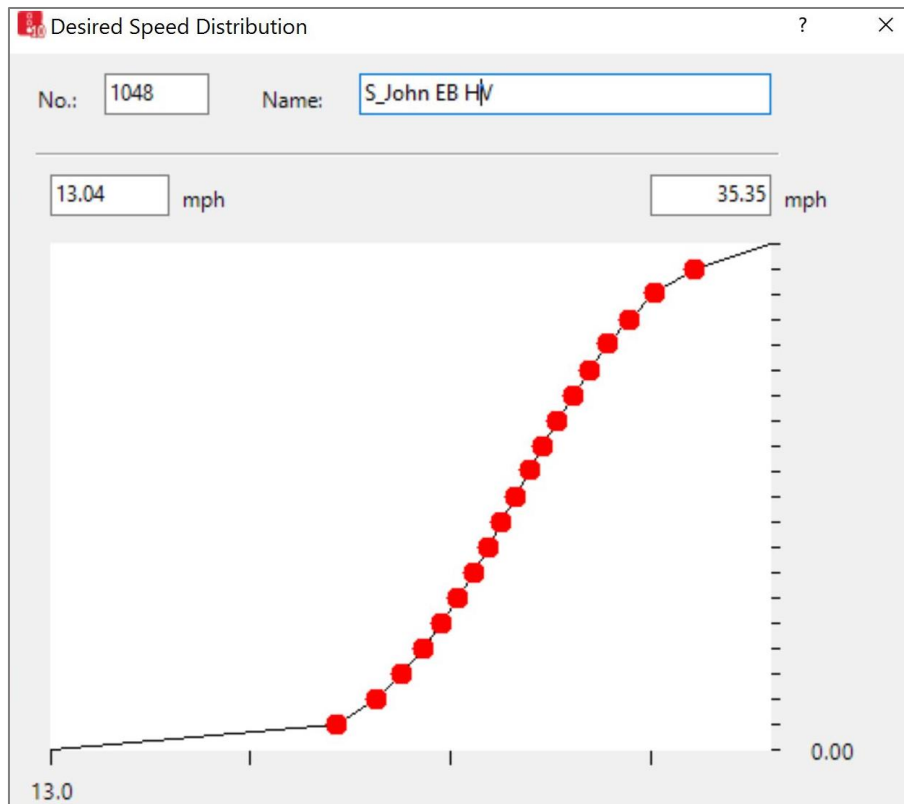


Figure 4.11 - Desired Speed Distribution in VISSIM

Furthermore, data collection points were added to the simulation network in order to get traffic information data from VISSIM. To extract traffic data, they were installed near the intersections and sometimes in the middle of the roadway segments. Data collection points recorded times when the front and rear of a car reached and left a point, respectively, vehicle type, speed, acceleration, etc. One data collection point can only record one lane of traffic information. Therefore, if a roadway segment has multiple lanes, then multiple detectors are needed. Figure 4.12 shows the detail of data collection points in VISSIM. The name indicates roadway segments (eastbound (EB) or westbound (WB)), and the data collection points indicate how many points or lanes are present in that segment.

Start page		Network Editor	
Data Collection Measurements			
Select layout... <Single List>			
Coun	No	Name	DataCollectionPoints
1	1	IN_Dr_EB	1,2
2	2	IN_Dr_NB	3,4
3	3	IN_Dr_SB	5,6
4	4	IN_Dr_WB	7,8
5	5	Millenia_EB	9,10
6	6	Milenia_SB	11,12
7	7	Millenia_WB	13,14
8	8	EB_After_Millenia	15,16
9	9	WB_after_Millenia	17,18
10	10	Harcout_EB	19,20

Figure 4.12 - Data Collection Points in VISSIM

4.2.4 VISSIM Network

The full micro simulation network so far developed in VISSIM is given below (Figure 2.13):

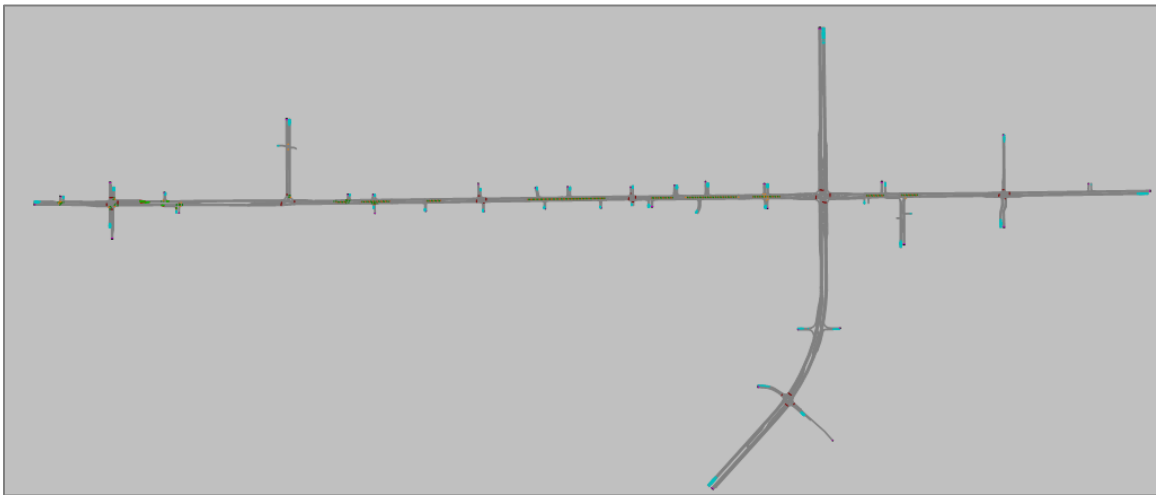


Figure 4.13 - Microsimulation Network in VISSIM

4.3 Calibration

Traffic data like volume and travel time were aggregated into five-minute intervals for calibration purposes. The simulation time was from 7:00 to 9:00 a.m., and the first and last 30 minutes were selected for warm-up and cool-down periods. One of the major roadway

geometry features in the school zone was a TWLTL for multiple driveway access. In VISSIM, TWLTL was incorporated just like the real field.

The Geoffrey E. Heavers (GEH) statistic is a modified Chi-square statistic that incorporates both relative and absolute differences and was used to compare between field and simulated traffic volumes. The definition of GEH is as follows:

$$GEH = \sqrt{\frac{2(V_{obs}(n) - V_{sim}(n))^2}{(V_{obs}(n) + V_{sim}(n))}} \dots\dots\dots(5.1)$$

where $V_{obs}(n)$ is the hourly observed volume of field detectors and $V_{sim}(n)$ is the hourly simulated volume obtained from the simulation network. The simulated volume replicates the field volume perfectly if the GEH value is less than 5 for 85% cases [28, 29, 30]. Also, to measure the goodness of fit, the correlation coefficient (CC) was calculated, which indicates the degree of linear association between field and simulated volumes. The definition of CC is given below:

$$CC = \frac{1}{n-1} \sum_{i=1}^n \frac{(y_{i,sim} - \hat{y}_{sim})(y_{i,obs} - \hat{y}_{obs})}{S_{sim}S_{obs}} \dots\dots\dots(5.2)$$

where n is the total number of traffic measurement observations; \hat{y}_{sim} and \hat{y}_{obs} are the means of the simulation and observed measurements, respectively; and S_{sim} and S_{obs} are the standard deviations of the simulated and observed measurements respectively. A CC value of 1 shows a perfect and direct correlation, while -1 shows a perfect and inverse relationship [31, 32,33]. A CC value of 0.85 is considered acceptable for the model calibration [32]. Another measure that gives information on the relative error is Theil's inequality coefficient, given by:

$$U = \frac{\sqrt{\frac{1}{n} \sum_{i=1}^n (y_{i,obs} - y_{i,sim})^2}}{\sqrt{\frac{1}{n} \sum_{i=1}^n (y_{i,obs})^2 + \frac{1}{n} \sum_{i=1}^n (y_{i,sim})^2}} \dots\dots\dots(5.3)$$

where n is the number of observations, and $y_{i,obs}$ and $y_{i,sim}$ are the overserved and simulated values at time i , respectively. U is the Theil's inequality coefficient, which is bounded between zero and one ($U=0$ implies a perfect fit between the observed and simulated measurements) [33]. To compare with the field condition, traffic volume was aggregated into 5-minute intervals and ten simulations were run with different random seeds to capture the randomness effect. Finally, the average of the ten simulations was used for the analysis. Results showed that in more than 89% cases, the GEH value was less than 5 and in around 99% cases, the GEH value was less than 10. The CC value is 0.96, which indicates a perfect and direct

correlation. Also, Theil's inequality coefficient was 0.08, which means the error is very small and there is a perfect fit between the simulated and observed volumes.

For validating the network, the difference between the field and simulated travel time should be within ± 1 minute for routes with observed travel times less than seven minutes and within $\pm 15\%$ for routes with observed travel times greater than seven minutes for all routes identified in the data [32]. Even though the travel time was less than seven minutes for all cases in this research project, both criteria were used for travel time validation. Hence, the result showed that in 100% of cases, the simulated travel time and the field travel time differences were less than 1 minute, and in 87.5% of cases, the differences between the observed and simulated travel time were less than 15%. Also, the default values of the VISSIM following parameters were changed, but there was no significant difference between the default and modified parameter results. So, after calibration with volume and validation with travel time, there was no significant difference between the field and simulation in terms of volume and travel time.

5 Proposed Methodologies

In order to assess the safety performance of different roadway characteristics in school zones, this research project tested three different countermeasures: two-step speed reduction (TSR), decreasing the number of driveways, and converting the TWLTL to a raised median. Also, the combination of best measures was tested to observe the safety effect in the school zones.

5.1 Two-Step Speed Reduction (TSR)

Ellison et al. [5] showed that if the speed of the previous segment is higher than 70 km/h, then it is difficult to reduce the speed to the posted speed limit (40 km/h). Thus, in this research project, an intermediate zone was provided for the smooth reduction of speed instead of sudden change from the higher speed limit of the upstream section to the lower speed limit near the school zone and captured how this TSR improves safety in the school zone.

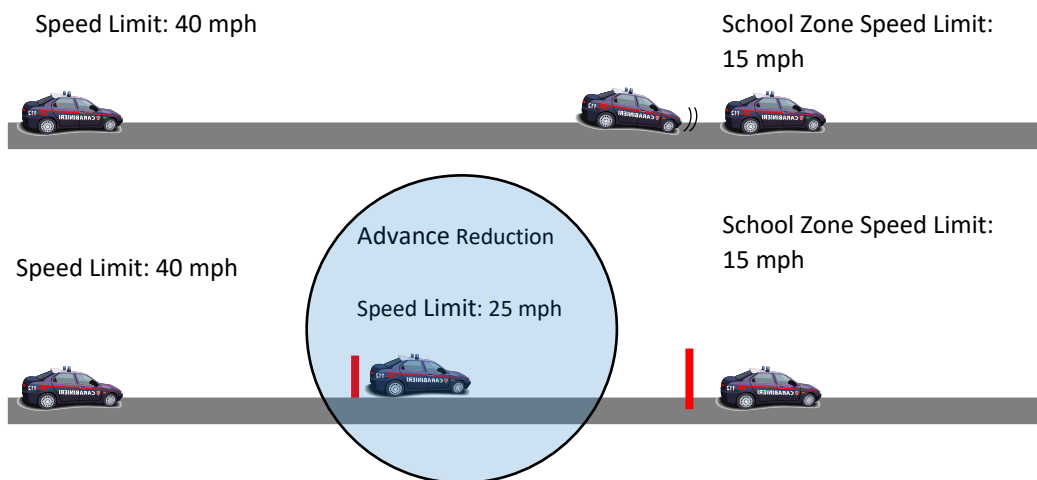


Figure 5.1 - Two-Step Speed-Reduction Procedure

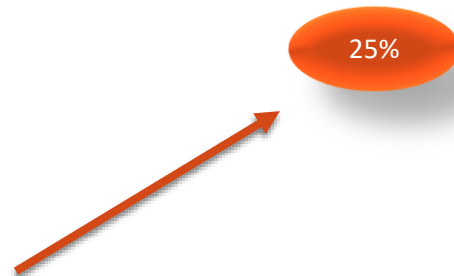
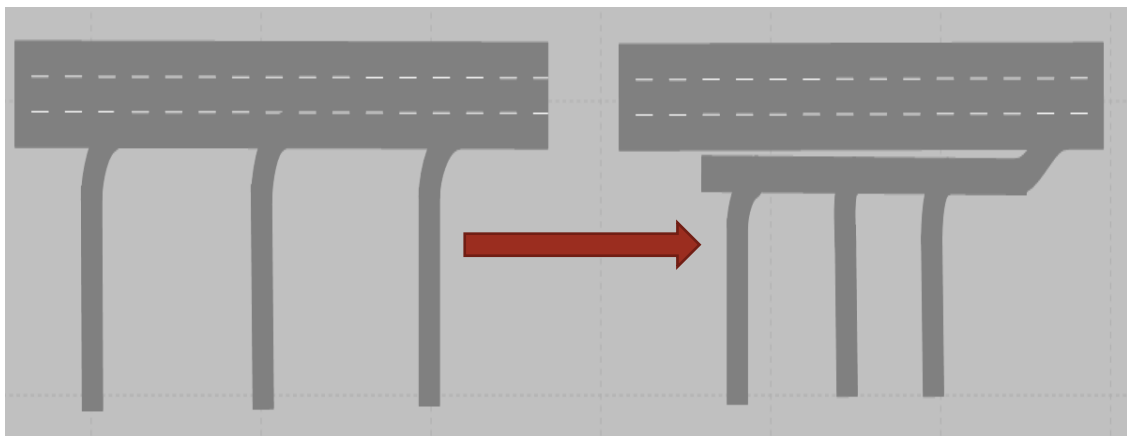
The first part of Figure 5.1 shows that the speed limit of the upstream section ahead of the school zone is 40 mph, which is reduced to 15 mph in the school zone during school hours. This variation might result in a higher standard deviation of speed and increase the probability of rear-end crash occurrence. In order to address this problem, an advance speed reduction zone (second part of Figure 2) was created between the high and low speed limit zone so that drivers can reduce speed slowly instead of suddenly changing speed from the upstream section to the school zone. Depending on the maximum speed limit (40 mph) on the main roadway, three different procedures of TSR (sub-scenarios) were tested in microsimulation:

- i. 40-25-15 [maximum speed limit 40 mph, advance reduction 25 mph, and school zone speed limit 15 mph]
- ii. 40-20-15 [maximum speed limit 40 mph, advance reduction 20 mph, and school zone speed limit 15 mph]
- iii. 40-30-15 [maximum speed limit 40 mph, advance reduction 30 mph, and school zone speed limit 15 mph]

5.2 Decreasing the Number of Driveways (DD)

As the land use pattern near the study area was more like residential, there were too many driveway accesses connected with the main road. This increased number of driveway accesses might increase the crash frequency near the school zone area [34]. Therefore, the number of driveway accesses was reduced gradually by 25, 50, 75, and 100 percent by connecting them with the main road through a collector road in order to test how this change affects safety in the school zone. Four sub-scenarios (Figure 6.13) were introduced under this measure:

- i. DD 25% [driveways reduced by 25%]
- ii. DD 50% [driveways reduced by 50%]
- iii. DD 75% [driveways reduced by 75%]
- iv. DD 100% [driveways reduced by 100%]



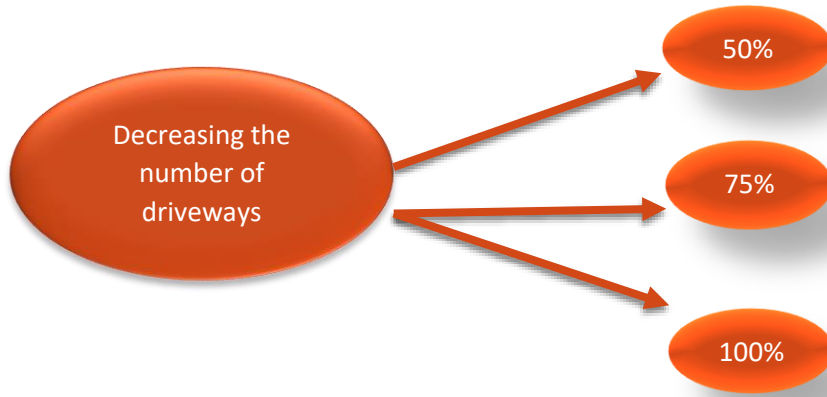


Figure 5.2 - Reducing Driveway Access

5.3 Replace TWLTL with Raised Median (RM)

There were too many TWLTLs in the study area for access between the driveway and the main road, which might create confusion for drivers during turning and result in a severe crash. Therefore, the TWLTL was replaced by a raised median (RM) (Figure 5.3) to measure how this change improves safety in the school zone. Because the TWLTL was replaced by a RM, vehicles need to make a U-turn at either the intersection or the median to reach their desired location. So, we tested two sub-scenarios in this case: (1) Intersection U-turn, and (2) Median U-turn.

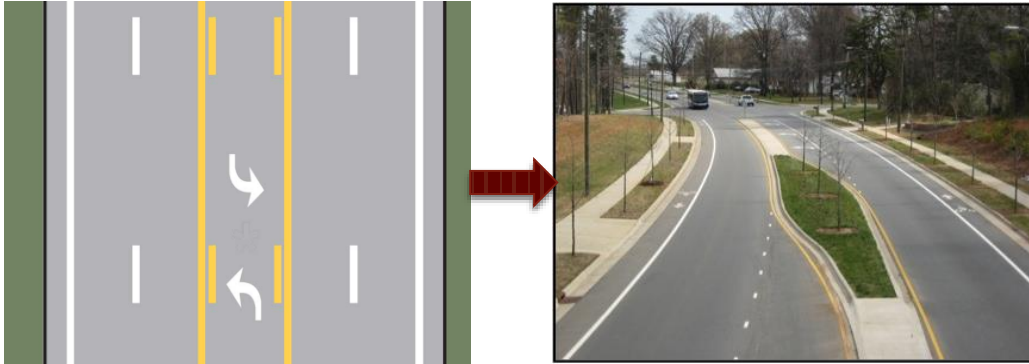


Figure 5.3 - TWLTL to Raised Median

6 Surrogate Measures of Safety

The surrogate measures of safety are widely used as indicators to evaluate crash risk in the microsimulation software as it cannot be directly used to measure crashes or traffic safety. Thus, the surrogate measures of safety are used as an alternative to evaluate the crash risk in microsimulation. In previous studies [35, 36], lots of surrogate safety measures, i.e., time-to-collision, post-encroachment time, and rear-end crash risk index, etc., were used. In this research project, three surrogate measures of safety were considered. Two advanced surrogate safety measures were developed from TTC notations and denoted as TET and TIT to evaluate traffic safety in school zones. The TTC concept was first introduced by Hayward [37] and is defined as the time that remains until a collision between two vehicles (following and leading) would occur if the collision course and speed difference were maintained. A smaller TTC value indicates a higher risk of collision at a certain time instant because it represents the time required for two successive vehicles moving in the same lane to collide if they continue at the same speed, where the following vehicle n is moving faster than the leading vehicle ($n-1$). This is expressed by:

$$TTC_n(t) = \begin{cases} \frac{y_{n-1}(t) - y_n(t) - L_{n-1}}{v_n(t) - v_{n-1}(t)}, & \text{if } v_n(t) > v_{n-1}(t) \\ \infty, & \text{if } v_n(t) \leq v_{n-1}(t) \end{cases} \dots\dots\dots(6.1)$$

where $TTC_n(t)$ = the TTC value of vehicle n at time t , y = the positions of vehicles, v = the velocities of vehicles, and L_{n-1} = Length of leading vehicles.

Previous studies [29,36] used two types of TTC for analyzing traffic safety; TTC1 denoted that the leading vehicle always maintains its current speed without any change, while TTC2 explained the situation where the leading vehicle stops suddenly. The latter is called TTC at brake (TTC_{brake}). In this research project, we analyzed both TTC1 and TTC2, but TTC2 is more appropriate as traffic data was collected from several detectors in VISSIM. The TTC at brake is defined as follows:

$$TTC_{brake}(t) = \frac{y_{n-1}(t) - y_n(t) - L_{n-1}}{v_n(t)} \dots\dots\dots(6.2)$$

The TET and TIT are used to evaluate the risks of collision aggregately and were developed by Minderhoud and Bovy [38]. The TET expresses the total time spent in safety-critical situations, characterized by a TTC_{brake} value below the threshold value TTC^* :

$$TET(t) = \sum_{n=1}^N \delta_t \times \Delta t, \quad \delta_t = \begin{cases} 1, & 0 < TTC_{brake}(t) \leq TTC^* \\ 0, & \text{otherwise} \end{cases} \dots\dots\dots(6.3)$$

$$TET = \sum_{t=1}^{Time} TET(t) \dots\dots\dots(6.4)$$

where t = time ID, n = vehicle ID, N = total number of vehicles, δ = switching variable, Δt = time step, which was 0.1 s in simulation, Time = simulation period, and TTC^* = the threshold of TTC. In general, the values of TTC^* threshold vary from 1 to 3 s, which is used to differentiate between safe and unsafe car-following conditions [29,39].

The TIT is also defined by TTC_{brake} and TTC^* , which is given below:

$$TIT(t) = \sum_{n=1}^N \left[\frac{1}{TTC_{brake}(t)} - \frac{1}{TTC^*} \right] \cdot \Delta t, 0 < TTC_{brake}(t) \leq TTC^* \dots\dots\dots(6.5)$$

$$TIT = \sum_{t=1}^{Time} TIT(t) \dots\dots\dots(6.6)$$

A rear-end crash risk index (RCRI) was first proposed by Oh et al. [40]. A rear-end crash may occur when two vehicles are moving in the same lane and the leading vehicle stops suddenly but the following vehicle does not decelerate in time with the following vehicle. So, if the following distance between the leading and the following vehicle plus the stopping distance of the leading vehicle is smaller than the stopping distance of the following vehicle, then a rear-end crash may occur. In order to avoid the rear-end crash, the following vehicle should follow its leading vehicle by making a sufficient gap between them. According to Oh et al. [40], the RCRI can be expressed as:

$$SD_F > SD_L$$

$$SD_L = v_L \times h + \frac{v_L^2}{2 \times a_L} + l_L \dots\dots\dots(6.7)$$

$$SD_F = v_F \times PRT + \frac{v_F^2}{2 \times a_F} \dots\dots\dots(6.8)$$

where SD_L and SD_F are the stopping distance of the leading and the following vehicles, respectively; PRT is the perception-reaction time; h is the time headway; l_L is the length of the leading vehicle; v_L is the speed of the leading vehicle; v_F is the speed of the following vehicle; a_L is the deceleration rate of the leading vehicle; and a_F is the deceleration rate of the following vehicle. Furthermore, Rahman and Abdel-Aty [28] proposed a new surrogate safety measure derived from RCRI and denoted as TERCRI, which is defined as:

$$TERCRI(t) = \sum_{n=1}^N RCRI_n(t) \times \Delta t, RCRI_n(t) = \begin{cases} 1, & SD_F > SD_L \\ 0, & \text{Otherwise} \end{cases} \dots\dots\dots(6.9)$$

$$TERCRI = \sum_{t=1}^{Time} TERCRI(t) \dots\dots\dots(6.10)$$

In VISSIM, we used three types of vehicles: PCs, HVs, and SBs. Therefore, for estimating the reliable safe distance for the leading and following vehicles, different deceleration rates were employed in this research project. The deceleration rate of PCs was selected as 3.42 m/s², and for both HGVs and SBs, the rate was 2.42 m/s². The value of PRT was used as 1.5 s, which is accepted by AASHTO [411].

In this research project, we analyzed these three surrogate safety measures for all scenarios and compared them.

7 Results and Discussion

As mentioned earlier, we introduced three countermeasures: two-step speed reduction, decreasing the number of driveways, and replacing TWLTL with RM. We analyzed TET, TIT, and TERCRI for each measure, which was further compared with the field condition (base scenario). Each sub-scenario was simulated 30 times in order to consider the randomness effect of simulation. At first, the TTC threshold was considered to be 1.5 seconds and further sensitivity analysis was conducted for different values of TTC thresholds from 1 to 3 seconds. The descriptive statistics of the three surrogate safety measures (TET, TIT, and TERCRI) for all sub-scenarios are presented in Tables 7.1 and 7.2. Also, the average value of all sub-scenarios is shown in Figure 7.1.

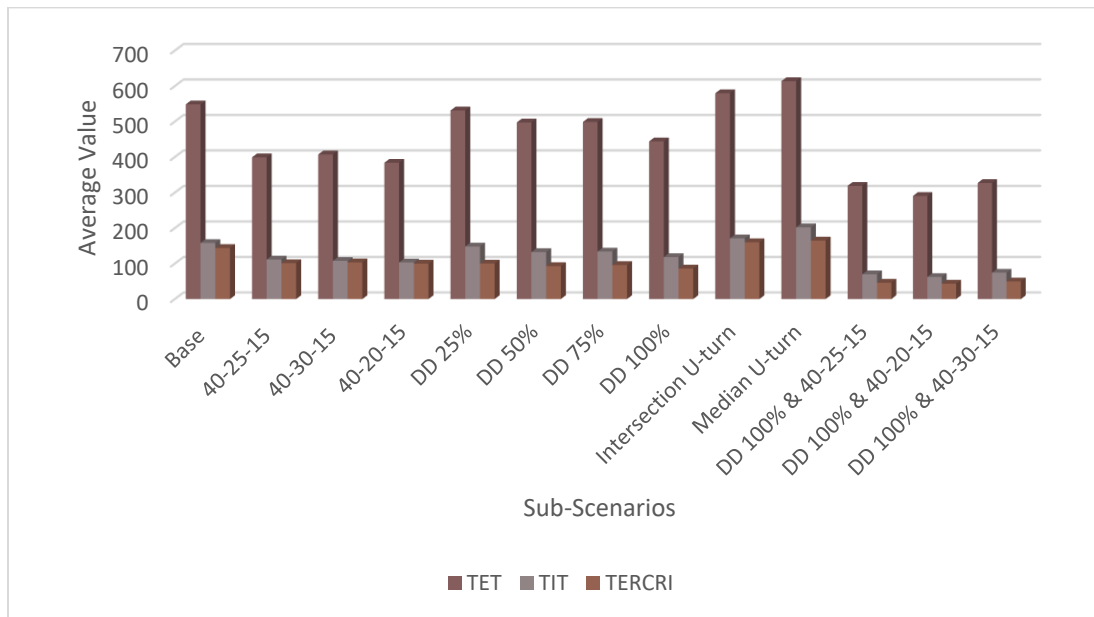


Figure 7.1 - Average Value of TET, TIT and TERCRI for All Sub-scenarios.

The higher values of TET, TIT, and TERCRI imply more dangerous situations. Thus, the result showed that the crash risk is higher for the base scenario than for all sub-scenarios, except for converting TWLTL to RM. For TSR, the 40-25-15 and 40-20-15 sub-scenarios showed the best result among the three, while for DD, the value of the surrogate safety measures decreases with the increase of the reduction percentage of the number of driveways (Figure 7.1).

Table 7.1 - Summary Statistics of TET and TIT

TET					
Scenarios	Sub-Scenario	Mean(s)	Std Dev(s)	Minimum(s)	Maximum(s)
Base	Base	548	43	444	620
Two-step speed Reduction	40-25-15	399	31	332	448
	40-30-15	407	31	337	457
	40-20-15	384	30	321	437
Decreasing the number of Driveways	DD 25%	531	45	432	612
	DD 50%	498	39	416	569
	DD 75%	499	37	428	557
	DD 100%	444	31	383	497
TWLTL to RM	Intersection U-turn	580	41	486	662
	Median U-turn	614	42	520	685
DD and TSR	DD 100%& 40-25-15	319	27	263	380
	DD 100%& 40-20-15	291	25	239	352
	DD 100%& 40-30-15	327	26	276	383
TIT					
Base	Base	158	40	113	345
Two-step speed Reduction	40-25-15	112	27	86	218
	40-30-15	108	10	91	130
	40-20-15	103	25	83	204
Decreasing the number of Driveways	DD 25%	148	16	117	200
	DD 50%	132	12	111	157
	DD 75%	134	10	117	153
	DD 100%	118	10	100	144

TWLTL to RM	Intersection U-turn	171	15	138	206
	Median U-turn	202	104	156	735
DD and TSR	DD 100%& 40-25-15	70	7	54	86
	DD 100%& 40-20-15	62	8	52	85
	DD 100%& 40-30-15	74	7	61	91

On the other hand, for TWLTL to RM, all the three measures for both sub-scenarios were higher than for the base scenario, which indicates a higher probability of crash risk than the field condition. Also, the standard deviation of TET, TIT, and TERCRI was higher for the base scenario than for all other sub-scenarios of TSR and DD, which are presented in Tables 7.1 and 7.2, respectively.

Moreover, we combined the best sub-scenarios (combinations of DD 100% with 40-25-15, 40-20-15, 40-30-15, separately) based on the above results for analyzing surrogate safety measures and found that all three combined sub-scenarios outperformed all other sub-scenarios. The minimum, maximum, mean, and standard deviation of the TET, TIT, and TERCRI values for the three combined sub-scenarios were very low compared to the base scenario, as shown in Tables 7.1 and 7.2.

Table 7.2 - Summary Statistics of TERCRI

Scenarios	Sub-Scenario	Mean (s)	Std Dev (s)	Minimum (s)	Maximum (s)
Base	Base	144	10	123	161
Two-step speed Reduction	40-25-15	101	6	91	113
	40-30-15	103	6	91	115
	40-20-15	100	6	89	111
Decreasing the number of Driveways	DD 25%	88	6	77	103
	DD 50%	93	7	79	108
	DD 75%	99	7	86	113
	DD 100%	86	7	75	100
	Intersection U-turn	160	9	143	176

TWLTL to RM	Median U-turn	165	9	147	183
DD and TSR	DD 100% & 40-25-15	46	4	39	58
	DD 100% & 40-20-15	44	4	38	56
	DD 100% & 40-30-15	50	4	43	65

A one-way ANOVA analysis was also conducted for all thirteen sub-scenarios, as shown in Table 7.3. The F-values for TET, TIT, and TERCRI were 265.89, 44.47, and 870.54, respectively, which are considerably higher than the critical values at 95% confidence level. Therefore, we can conclude that there are significant differences among the thirteen sub-scenarios, including the base. Moreover, we tested ANOVA separately for TSR, DD, TWLTL to RM, and the combination of DD and TSR. The results indicated that the sub-scenarios are also significantly different from each other.

In addition, the distributions of TET, TIT, and TERCRI for four sub-scenarios, i.e., base, 40-25-15, DD 100%, and DD 100% & 40-25-15 are shown in Figures 7.2(a), 7.2(b), and 7.2(c), respectively.

Table 7.3 - One-Way ANOVA Analysis of TET, TIT, and TERCRI.

Measures	Attribute	Sum of squares	d.f.	Mean Squares	F-value	p-value
TET	Between Groups	3935360	12	327947	265.89	<0.0001
	Within Groups	464995	377	1233.408		
	Total	4400355	389			
TIT	Between Groups	609480	12	50790	44.47	<0.0001
	Within Groups	430532	377	1142		
	Total	1040012	389			
TERCRI	Between Groups	569215	12	47435	870.54	<0.0001
	Within Groups	19373	377	51		
	Total	588588	389			

Furthermore, the mean value of TET, TIT, and TERCRI for these four sub-scenarios are presented in Figure 7.2 (d), which shows that all three sub-scenarios improved considerably compared to the base scenario but that the combined sub-scenarios (DD 100% & 40-25-15) reduced TET, TIT, and TERCRI values more (by approximately 42%, 56%, and 68%, respectively) than the base scenario.

The above results of TET and TIT are mainly based on the same parameter setting of TTC threshold of 1.5 s. A sensitivity analysis of TTC thresholds was also conducted for all thirteen sub-scenarios, but only the best three sub-scenarios are presented in Table 7.4.

Table 7.4 - Sensitivity Analysis of Different Values of TTC Threshold

TTC* (s)	Sub-Scenarios	Base		Sub-Scenarios 1 (DD 100%)		Sub-Scenarios 2 (40-25-15)		Sub-Scenarios 3 (DD 100% & 40-25-15)	
		TET(s)	TIT(s)	TET(s)	TIT(s)	TET(s)	TIT(s)	TET(s)	TIT(s)
1.5	Average value	549	158	444	118	399	112	319	70
	Changing proportion	-	-	19%	25%	27%	29%	42%	56%
2.0	Average value	772	269	678	211	648	218	581	143
	Changing proportion	-	-	12%	21%	16%	19%	25%	47%
3.0	Average value	1001	416	905	343	931	349	863	264
	Changing proportion	-	-	10%	18%	7%	16%	14%	37%

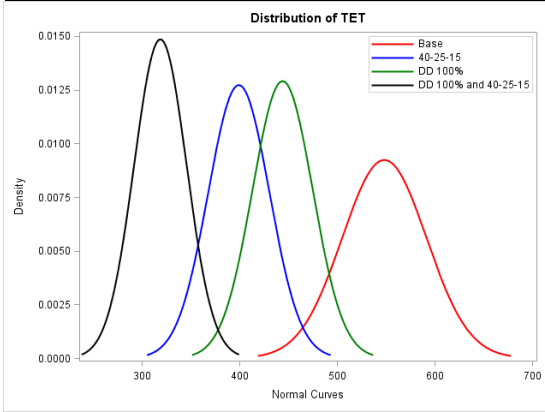
The results show that, compared with the base scenario, all the reductions of TET and TIT values maintain within 35% to 7% and 24% to 16%, respectively, for Scenario 1. For Scenario 2, those relative reductions of TET and TIT were 19% to 10% and 25% to 17%, respectively. Also, TET and TIT values were reduced more for Scenario 3 (42% to 14% and 56% to 37%, respectively). Lastly, for each value of TTC threshold, TET and TIT reduction percentage increased from Sub-scenario 1 to Sub-scenario 3. The sensitivity analysis of all thirteen scenarios for TET and TIT separately is given below:

Table 7.5 - Sensitivity Analysis of TET

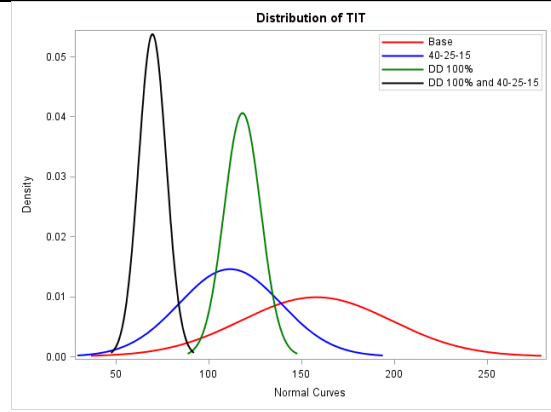
TTC Threshold (s)	40-25-15	40-30-15	40-20-15	DD 25%	DD 50%	DD 75%	DD 100%	DD 100% +40-25-15	DD 100%+ 40-20-15	DD 100% +40-30-15
1	34.6	31.8	37.4	3.2	5.0	1.5	18.2	57.3	63.5	52.9
1.5	27.2	25.7	30.0	3.2	9.3	9.0	19.0	41.8	47.0	40.4
2	16.1	15.3	17.2	5.9	12.8	13.4	12.2	24.8	26.9	24.0
2.5	9.8	9.4	10.7	5.7	12.3	13.2	9.8	16.8	18.3	16.3
3	7.0	6.7	7.6	5.3	11.6	12.5	9.6	13.8	15.1	13.5

Table 7.6 - Sensitivity Analysis of TIT

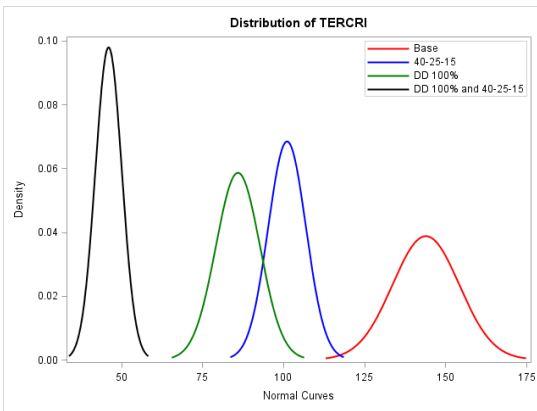
TTC Threshold (s)	40-25-15	40-30-15	40-20-15	DD 25%	DD 50%	DD 75%	DD 100%	DD 100% +40-25-15	DD 100%+ 40-20-15	DD 100% +40-30-15
1	24.1	37.0	33.2	21.6	39.0	35.8	39.6	70.0	70.5	68.1
1.5	29.4	31.7	34.7	6.3	16.2	15.2	25.2	55.8	60.6	52.9
2	18.9	2.3	30.0	5.8	14.4	14.0	21.4	46.7	50.8	44.5
2.5	17.4	2.8	26.1	5.8	14.0	13.9	18.8	40.4	43.9	38.6
3	16.0	3.6	23.5	5.8	13.7	13.7	17.4	36.6	39.8	35.0



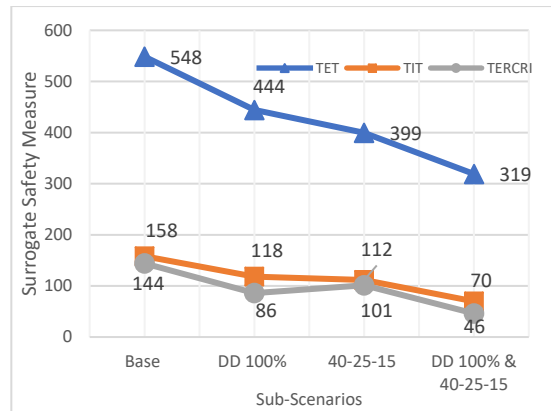
(a)



(b)



(c)



(d)

Figure 7.2 - Distribution of TET (a), TIT (b), TERCRI (c) for the Best Three Sub-scenarios with Base Scenarios and the Value of TET, TIT, TERCRI for the Best Three Sub-scenarios with Base Scenario (d).

8 Summary and Conclusion

The main objective of this research project was to propose different countermeasures for school zones and evaluate them by using microsimulation. First, the most crash-prone school zone was identified based on crash rates and was further analyzed by VISSIM. The simulation experiments were designed by deploying sub-scenarios of three countermeasures (TSR, DD, and replacing TWLTL with RM), and three surrogate safety measures (TET, TIT, and TERCRI) were analyzed for all sub-scenarios separately, as were their combined effects.

The results indicated that the implementation of TSR and DD significantly improved safety in the school zones. The values of TET, TIT, and TERCRI were larger for the base scenario than for all other sub-scenarios except converting TWLTL to RM. In TWLTL to RM, two sub-scenarios were tested and showed a larger value of surrogate safety measures than the base scenario because of the large amount of traffic that made a U-turn both at the intersection and median. Moreover, the combined scenarios of TSR and DD outperformed all other scenarios. One-way ANOVA analysis showed that there was a significant difference among all thirteen sub-scenarios. Furthermore, the sensitivity analysis indicated that different values of TTC thresholds do not affect the results.

9 Follow-up Research Topics

Although this research project proposed multiple countermeasures to improve traffic safety at school zones and confirmed their effectiveness, there are important issues that remain to be investigated in follow-up studies. For DD scenarios, vehicles could not directly access the main road because they had to use the collector road first, and for the TWLTL to RM scenarios, vehicles had to use the intersection or median U-turn instead of using the center lane (TWLTL) for left turning movements. So, this might create some delay, which is not addressed in this research project. Thus, it is worth studying how to capture the delay. In addition, more innovative countermeasures that could improve traffic safety in school zones have been proposed and should be evaluated. Also, additional research is needed to evaluate pedestrian and bicycle safety in school zones.

Moreover, connected vehicles (CV) technology has recently drawn increasing attention from researchers and is regarded as one of the most promising methods to improve traffic safety. Some previous studies [29] evaluated traffic safety under CV technology and analyzed the market penetration rate of CV technology. Thus, the application of CV technology in school zones to enhance traffic safety could be a potential extension to this research.

References

1. Peden, M., Scurfield, R., Sleet, D., Mohan, D., Hyder, A.A., Jarawan, E., Mathers, C., 2004. World report on road traffic injury prevention, World Health Organization. doi:10.1016/j.puhe.2005.09.003.
2. Roper, P., Thoresen, T., Tziotis, M., Imberger, K., 2006. Evaluation of flashing lights in 40 km/h school speed zones. Sydney, Aust. ARRB Consult.
3. Abdel-Aty, M., Chundi, S.S., Lee, C., 2007a. Geo-spatial and log-linear analysis of pedestrian and bicyclist crashes involving school-aged children. *J. Safety Res.* 38 5 , 571–579. doi:10.1016/j.jsr.2007.04.006
4. Warsh, J., Rothman, L., Slater, M., Steverango, C., Howard, A., 2009. Are school zones effective? An examination of motor vehicle versus child pedestrian crashes near schools. *Inj. Prev.* 15 4 , 226–229. doi:10.1136/ip.2008.020446
5. Ellison, A.B., Greaves, S., Daniels, R., 2013. Capturing speeding behaviour in school zones using GPS technology. *Road Transp. Res.*
6. Kattan, L., Tay, R., Acharjee, S., 2011. Managing speed at school and playground zones. *Accid. Anal. Prev.* 43 5 , 1887–1891. doi:10.1016/j.aap.2011.04.009
7. McCoy, P.T., Heimann, J.E., 1990. School Speed Limits and Speeds in School Zones. *Transp. Res. Rec.*
8. Kirmizioglu, E., Tuydes-Yaman, H., 2012. Comprehensibility of traffic signs among urban drivers in Turkey. *Accid. Anal. Prev.* 45, 131–141. doi:10.1016/j.aap.2011.11.014
9. Saibel, C., Salzberg, P., Doane, R., Moffat, J., 1999. Vehicle speeds in school zones. *ITE J. (Institute Transp. Eng.* 69 11 , 38–42.
10. Hawkins, H.G., 2007. Rear-facing school speed limit beacons. *ITE J. (Institute Transp. Eng.* 77 6 , 18–23.
11. Gregory, B., Irwin, J.D., Faulks, I.J., Chekaluk, E., 2016. Differential effects of traffic sign stimuli upon speeding in school zones following a traffic light interruption. *Accid. Anal. Prev.* 86, 114–20. doi:10.1016/j.aap.2015.10.020
12. Simpson, C.L., 2008. Evaluation of Effectiveness of School Zone Flashers in North Carolina. *Transp. Res. Rec. J. Transp. Res. Board* 2074 1 , 21–28. doi:10.3141/2074-03
13. Lee, C., Lee, S., Choi, B., Oh, Y., 2006. Effectiveness of Speed-Monitoring Displays in Speed Reduction in School Zones. *Transp. Res. Rec. J. Transp. Res. Board* 1973, 27–35. doi:10.3141/1973-06
14. Ash, K.G., Saito, M., 2006. Field Evaluation of the Effect of Speed Monitoring Displays on Speed Compliance in School Zones, in: *Applications of Advanced Technology in Transportation*. American Society of Civil Engineers, Reston, VA, pp. 780–786. doi:10.1061/40799(213)125
15. Ullman, G., Rose, E., 2005. Evaluation of Dynamic Speed Display Signs. *Transp. Res. Rec. J. Transp. Res. Board* 1918, 92–97. doi:10.3141/1918-12
16. Freedman, M., De Leonardis, D., Raisman, G., InyoSwan, D., Davis, A., Levi, S., Rogers, I., Bergeron, E., 2006. Demonstration of automated speed enforcement in school zones in Portland, Oregon. United States. National Highway Traffic Safety Administration.
17. Zhao, X., Li, J., Ma, J., Rong, J., 2016. Evaluation of the effects of school zone signs and markings on speed reduction: a driving simulator study. *Springerplus* 5 1 , 789. doi:10.1186/s40064-016-2396-x
18. Pucher, J., Renne, J.L., 2005. Rural mobility and mode choice: Evidence from the 2001

- National Household Travel Survey. Transportation (Amst). doi:10.1007/s11116-004-5508-3
19. Clifton, K.J., Kreamer-Fults, K., 2007. An examination of the environmental attributes associated with pedestrian-vehicular crashes near public schools. *Accid. Anal. Prev.* doi:10.1016/j.aap.2006.11.003
 20. Ben-Bassat, T., Shinar, D., 2011. Effect of shoulder width, guardrail and roadway geometry on driver perception and behavior. *Accid. Anal. Prev.* 43 6 , 2142–52. doi:10.1016/j.aap.2011.06.004
 21. Tay, R., 2009. Speed Compliance in School and Playground Zones. *Ite Journal-Institute Transp. Eng.* 79 3 , 36–38.
 22. Strawderman, L., Rahman, M.M., Huang, Y., Nandi, A., 2015. Driver behavior and accident frequency in school zones: Assessing the impact of sign saturation. *Accid. Anal. Prev.* doi:10.1016/j.aap.2015.05.026
 23. Burritt, B.E., Buchanan, R.C., Kalivoda, E.I., 1990. School zone flashers. Do they really slow traffic. *ITE J. (Institute Transp. Eng.* 60 1 , 29–31.
 24. Dowling, R., A. Skabardonis, and V. Alexiadis. Traffic Analysis Toolbox Volume III : Guidelines for Applying Traffic Microsimulation Modeling Software. Rep. No. FHWA-HRT-04-040, U.S. DOT, Federal Highway Administration, Washington, D.C, Vol. III, No. July, 2004, p. 146.
 25. PTV, 2016. PTV VISSIM 9 User Manual 1055.
 26. Hjalmdahl, M., Várhelyi, A., 2004. Speed regulation by in-car active accelerator pedal. *Transp. Res. Part F Traffic Psychol. Behav.* 7 2 , 77–94. doi:10.1016/j.trf.2004.02.002
 27. Hallmark, S.L., Isebrands, H., 2005. Evaluating speed differences between passenger vehicles and heavy trucks for transportation-related emissions modeling. *J. Air Waste Manag. Assoc.* doi:10.1080/10473289.2005.10464742
 28. Abdel-Aty, M., Wang, L., 2017. Implementation of Variable Speed Limits to Improve Safety of Congested Expressway Weaving Segments in Microsimulation. *Transp. Res. Procedia* 27, 577–584. doi:10.1016/j.trpro.2017.12.061
 29. Rahman, M.S., Abdel-Aty, M., 2018. Longitudinal safety evaluation of connected vehicles' platooning on expressways. *Accid. Anal. Prev.* 117 December , 381–391. doi:10.1016/j.aap.2017.12.012
 30. Salceda, R., Martinez, M.T., 1992. Characterization of acetylcholinesterase and butyrylcholinesterase activities in retinal chick pigment epithelium during development. *Exp. Eye Res.* 54 1 , 17–22. doi:10.1016/j.trc.2014.05.016
 31. El Esawey, M., Sayed, T., 2011. Calibration and validation of micro-simulation models of medium-size networks. *Adv. Transp. Stud.* 24 , 57–76. doi:10.4399/97888548415126
 32. FDOT Systems Planning Office, 2014. Traffic Analysis Handbook. Florida Dep. Transp. March , 118.
 33. Hollander, Y., Liu, R., 2008. The principles of calibrating traffic microsimulation models. *Transportation (Amst).* 35 3 , 347–362. doi:10.1007/s11116-007-9156-2
 34. Park, J., Abdel-Aty, M., Lee, J. (2018). School Zone Safety Modeling in Countermeasure Evaluation and Decision. *Transportmetrica A: Transport Science*, In-Press.
 35. Abdel-Aty, M., Pande, A., Lee, C., Gayah, V., Santos, C. Dos, 2007b. Crash Risk Assessment Using Intelligent Transportation Systems Data and Real-Time Intervention Strategies to Improve Safety on Freeways. *J. Intell. Transp. Syst.* 11 3 , 107–120. doi:10.1080/15472450701410395
 36. Peng, Y., Abdel-Aty, M., Shi, Q., Yu, R., 2017. Assessing the impact of reduced visibility on

- traffic crash risk using microscopic data and surrogate safety measures. *Transp. Res. Part C Emerg. Technol.* 74, 295–305. doi:10.1016/j.trc.2016.11.022
37. Hayward, J.C., 1972. Near-miss determination through use of a scale of danger. *Highw. Res. Rec.* doi:TTSC 7115
38. Minderhoud, M.M., Bovy, P.H.L., 2001. Extended time-to-collision measures for road traffic safety assessment. *Accid. Anal. Prev.* 33 (1) , 89–97.
39. Li, Y., Wang, W., Xing, L., Fan, Q., Wang, H., 2018. Longitudinal safety evaluation of electric vehicles with the partial wireless charging lane on freeways. *Accid. Anal. Prev.* 111 December 2017 , 133–141. doi:10.1016/j.aap.2017.11.036
40. Oh, C., Park, S., Ritchie, S.G., 2006. A method for identifying rear-end collision risks using inductive loop detectors. *Accid. Anal. Prev.* 38 2 , 295–301. doi:10.1016/j.aap.2005.09.009
41. American Association of State Highway and Transportation Officials (AASHTO), 2004. A policy on geometric design of highways and streets. Washington, D.C.